# EFFECT OF ALLOYING ELEMENTS ON HIGH-STRAIN-RATE BEHAVIOUR IN RECYCLED Al-Fe-Si SYSTEM ALLOYS

**Frode WESTVOLD[1], Bjørn ANDERSSON[1], Yngve LANGSRUD[1], Jon Dag EVENSEN[2]**

[1]SINTEF Materials Technology, Forskningsveien 1, 0314 Oslo, NORWAY
[2]Hydro Aluminium Holmestrand Rolling Mill, 3081 Holmestrand, NORWAY

**ABSTRACT** Aluminium sheet alloys were tensile tested at strain rates $10^{-3}$, 20 and 100 $s^{-1}$. The alloys were five variants of soft annealed AA1200A with various alloying elements (Fe, Si, Mn, Cu, Zn and Mg), all from a recycled metal base. When subjected to high strain rate, the materials yielded at lower flow stress, but further increase in strains resulted in flow stresses that were higher than those obtained at low strain rates. This improved work hardening led to a considerably higher level of elongation. Alloying variants with Zn and/ or Mg in solid solution accelerated the high strain rate effects.

**Keywords:** High strain rate, work hardening, tensile test, sheet aluminium

## 1. INTRODUCTION

At industrial forming of aluminium sheet products, the strain rates are normally in the 0.1-100 $s^{-1}$ range [1]. Information about mechanical properties of the materials is however most often acquired by conventional tensile testing at strain rates between 0.0001 and 0.1 $s^{-1}$. Most aluminium alloys are relatively unaffected by strain rate changes at room temperature and low strain rates, but at the strain rates dominating in forming operations, a profound effect on strength and ductility has been demonstrated [2].

It is clear from previous work that the effect of strain rate is both alloy and temper dependent [2,3,4]. Few attempts have however been made to relate the observed behaviour to the microstructure and how various alloying elements effect the strength and ductility at different strain rates.

In this study, a fully annealed AA1200A sheet and four additional variants of the alloy with various levels of elements (Fe, Si, Mn, Cu, Zn and Mg) are used. These elements usually not part of the standard alloying composition or kept at low levels can be present in the recycled metal base and can considerably alter its properties. The variants have been tested at three different strain rates, i.e. a conventional strain rate of $10^{-3}$ $s^{-1}$ and the higher strain rates 20 and 100 $s^{-1}$. The object has been to reveal both how increased strain rate effects the properties of the materials in general, and eventually how the different elements effect the behaviour.

## 2. EXPERIMENTAL

### 2.1 Materials and processing

The chemical composition of the five different alloys is given in Table 1. The sheets were produced according to an industry-like thermo-mechanical laboratory process. After DC-casting the materials were cut and machined to plates of 15 mm thickness and 100 mm width. The materials were heated at ~100°C/h to a homogenising/ preheating temperature of 540°C with 6 hours holding time. The subsequent hot rolling reduced the plate thickness to 4 mm. The plates were cooled from

hot rolling temperature to room temperature in 22 hours to simulate an industrial coiling sequence. The sheets were then cold rolled to a final sheet thickness of 1 mm ± 0.07 mm and annealed at 100°C/h to 350°C with 3 hours holding time to ensure a fully recrystallised structure.

*Table 1. Composition of the alloys in wt%.*

| Alloy | Si | Fe | Mn | Cu | Zn | Mg | Others | Al |
|---|---|---|---|---|---|---|---|---|
| AA1200A | 0,16 | 0,48 | 0,10 | 0,03 | 0,05 | 0,11 | <0.05 | Balance |
| 1200+Fe+Si | **0,47** | **1,94** | 0,10 | 0,03 | 0,04 | 0,09 | " | " |
| 1200+Fe+Si+Mn | **0,48** | **1,85** | **0,48** | 0,03 | 0,04 | 0,10 | " | " |
| 1200+Fe+Si+Mn+Cu+Zn | **0,48** | **1,77** | **0,51** | **0,20** | **0,22** | 0,11 | " | " |
| 1200+Fe+Si+Mn+Cu+Zn+Mg | **0,50** | **1,84** | **0,48** | **0,20** | **0,22** | **0,30** | " | " |

### 2.2 Microstructural Characterisation

Optical metallography was utilised to characterise the microstructures. The linear intercept method was used to determine the grain size of the anodised specimens. A Jeol JSM-810 scanning electron microscope, with a LINK ISIS energy-dispersive X-ray analyser (EDS), was utilised to characterise primary particles. Transmission electron microscope (TEM) foils were prepared and thinned by jet polishing and subsequently analysed in a JEOL 200CX microscope.

Electrical conductivity measurements, to determine the level of elements in solid solution, were performed using a SIGMATEST D.

### 2.3 Mechanical Testing

A Zwick K250 static testing machine was used for test at crosshead speed of 2 mm/min. Tensile specimens with a 38 mm gauge length and a 6.35 mm width (DIN 50114) were machined in the longitudinal direction. This crosshead speed and sample geometry gave an initial strain rate of approximately $10^{-3}$ $s^{-1}$. Displacement and elongation were obtained from an extensometer attached to the specimen.

A Schenck Hydropuls VHS100/10 was used for ram speeds of respectively 1 m/s and 5 m/s. Tensile specimens with a 50 mm gauge length and a 22 mm width (modified ASTM E8) were machined in longitudinal direction for testing. This geometry and speed gave an initial strain rate of approximately 20 $s^{-1}$ and 100 $s^{-1}$, respectively. The load was measured using a piezoelectric crystal. Load and displacement data were transferred via an ADAM transient recorder to a computer. Because of oscillations in the signal, both the main oscillation and the material response were fitted to minimise the effect of the oscillations, and a curve-fitting program was utilised to reduce the unwanted disturbances. The material response was represented using a Voce equation $(\sigma = \sigma_0 + (\sigma_\infty - \sigma_0)(exp(-\varepsilon^b/\varepsilon_c)))$[5], were $\sigma_0$ is the initial flow stress, $\sigma_\infty$ the saturation stress, $\varepsilon_c$ a work hardening parameter and $b$ a coefficient. $b$ was used to give a good fit to the overall shape of the flow curve, and Considere's relation [6] was used as a constraint to ensure that the curvature of the flow stress at the uniform strain was correct. Total elongation was measured manually and uniform elongation, $\varepsilon_l$, was determined by measuring the elongation manually both in width, $\varepsilon_w$, and thickness direction, $\varepsilon_t$, over the test sample, using the relation $\varepsilon_l = -(\varepsilon_w + \varepsilon_t)$.

## 3. RESULTS

### 3.1 Microstructure

Optical microscopy of the alloys revealed the equiaxed grain sizes shown in table 2. The grain size appeared to decrease substantially with the addition of a near eutectic Fe to the base alloy. In the scanning electron microscope, primary precipitated particles containing Fe, Si, and Mn were observed, and their composition indicated the α-Al(Mn,Fe)Si phase. The size of these particles was in the 1-10 μm range, most of them between 1-2 μm. The density of primary particles was much

smaller in the base alloy, due to the lower level of Fe. The development of a fine grain structure by adding Fe is in accordance to previous knowledge. The effect is connected to Particle Stimulated Nucleation, where the coarse Fe-rich particles acts as nucleation sites for recrystallisation, and is utilised commercially in for example AA8006 and AA8011 alloys.

TEM analyses revealed that Mn, in addition to be part of the primary α-Al(Mn,Fe)Si particles, were present in the microstructure as dispersoids. In the Cu-rich alloys, Cu could be identified in small particles close to or on the primary particles. Mg and Zn in particles were not observed, in accordance to their high solubility in aluminium.

*Table 2. Grain size and electrical conductivity.*

| Alloy | Grain size [μm] | Electrical conductivity [MS/m] |
|---|---|---|
| AA1200A | 18±1 | 32.15±0.02 |
| 1200+Fe+Si | 11±1 | 31.48±0.02 |
| 1200+Fe+Si+Mn | 11±1 | 30.13±0.02 |
| 1200+Fe+Si+Mn+Cu+Zn | 12±1 | 29.19±0.03 |
| 1200+Fe+Si+Mn+Cu+Zn+Mg | 10±1 | 28.13±0.01 |

In Table 2 the electrical conductivity of the alloys is listed as well. The conductivity decreases with increasing alloying. By comparing the change in electrical conductivity, the conductivity-reducing effect of solid solution can be used to indicate the level of elements in solid solution [7]. This is however, not the main topic of the present work.

### 3.2 Mechanical testing

The mechanical properties of the tested alloys at low strain rate are given in Figure 1. Both yield stress and uniform stress increase by the addition of Fe and Si, probably due to a combination of grain size hardening and Si solid solution hardening. The elongation is not effected. Addition of Mn increases both yield strength and uniform stress, but reduces ductility. The additional strengthening mechanism seems to be dispersion hardening. Additions of Cu and Zn and also Mg do not effect the yield strength but increase the uniform strength. This is mainly due to better work hardening promoted by Cu and Mg, where Mg seems to have the strongest positive effect upon work hardening. The ductility decreases with increasing alloying content, especially for the Mg-rich alloy. Cu, Zn and Mn do not seem to have the same strong negative effect on elongation as Mg.

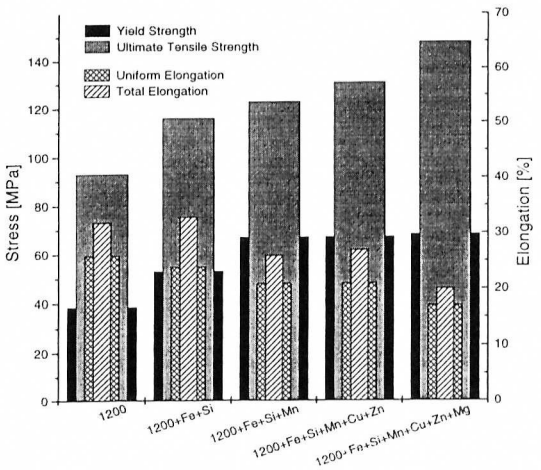


**Figure 1.** Mechanical testing at $\dot{\varepsilon} = 10^{-3}\ s^{-1}$.

The effect on stress /strain for the alloys at the three different strain rates is shown in Figure 2-5. True Stress-True Strain curves for *AA1200A+Fe+Si+Mn* are shown in Figure 2. They reveal strong strain rate dependence, and is representative for all the tested alloys. At low strains the level of flow stress is highest for the materials tested at low strain rate. As the strain increases this effect is reversed and the materials tested at high strain rates reach the highest stress level. Also, the uniform elongation increases with increasing strain rate.

The true ultimate tensile strength level at different strain rates is shown in Figure 3. The stress level is relatively unchanged from $10^{-3}$ to 20 $s^{-1}$, except from a slight positive effect for the three strongest alloys. From 20 to 100 $s^{-1}$, the stress level is increasing for all the alloys. True uniform strain shown in Figure 4 and total elongation shown in Figure 5 are both increasing between $10^{-3}$ and 20 $s^{-1}$. An exception is *1200+Fe+Si*, which displays relatively unchanged strain behaviour in this range. At strain rates between 20 and 100 $s^{-1}$, an increasing elongation with strain rate is observed.

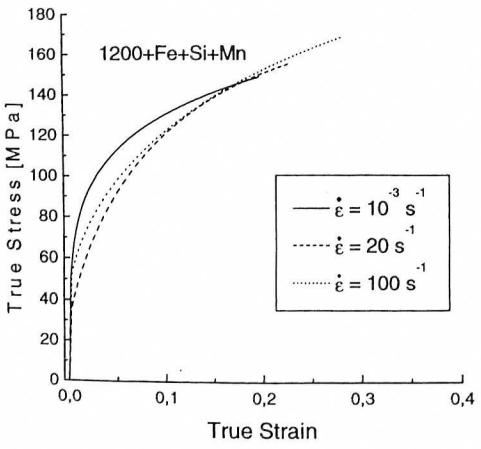


**Figure 2**. True stress-true strain curves for 1200+Fe+Si+Mn at $\dot{\varepsilon} = 10^{-3}$, 20, 100 $s^{-1}$.

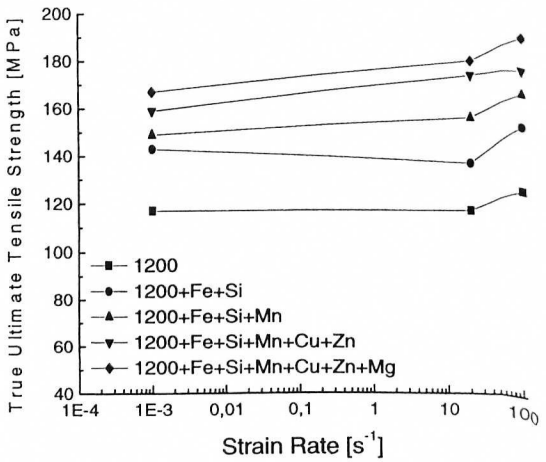


**Figure 3.** Effect of strain rate on ultimate tensile strength.

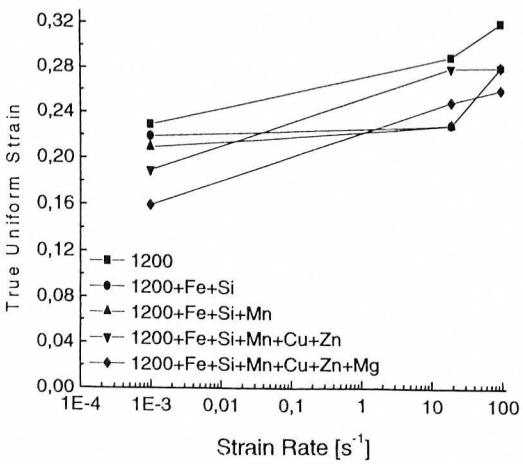


**Figure 4**. Effect of strain rate on uniform strain.

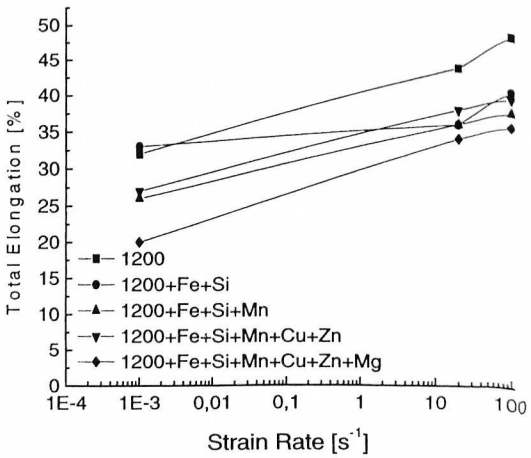


**Figure 5**. Effect of strain rate on total elongation.

The work hardening behaviour of the alloys at different strain ranges and strain rates is plotted in Figure 6. The work hardening is characterised by the factor $(\varepsilon/\sigma)^*(d\sigma/d\varepsilon)$ which is often called the instantaneous "n"-value, i.e. a variable n in the Holloman equation $\sigma = K\varepsilon^n$. General observations independent of alloying display at low strain rate a relatively constant work hardening over the strain range. At 20 $s^{-1}$ the work hardening is considerably higher at low strains compared to at high strains and the overall level of work hardening is higher than at lower strain rate. At 100 $s^{-1}$ the work hardening is higher at low strains than at high strain, but this difference is not as pronounced

as at 20 $s^{-1}$. The work hardening at low strain levels is lower at 100 $s^{-1}$ compared to 20 $s^{-1}$, but when reaching ultimate stress, the fastest strain rate provide the most effective work hardening.

At low strain rates, the work hardening is decreasing with increasing alloy content. At $\dot{\epsilon}$ = 20 $s^{-1}$ and 100 $s^{-1}$, the Cu/Zn and Mg rich alloys display the same work hardening at the two strain rates, whereas the other alloys show a work hardening behaviour towards uniform strain considerable lower at 20 $s^{-1}$ than 100 $s^{-1}$.

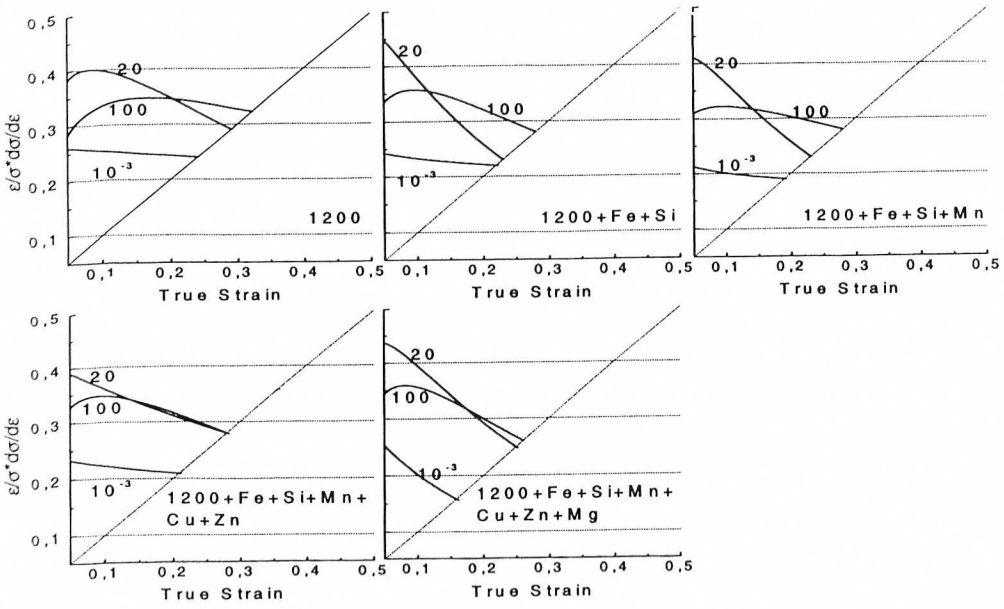


**Figure 6.** Instantaneous work hardening, ((ε/σ)*(dσ/dε)), as a function of strain at $\dot{\epsilon}$ = $10^{-3}$, 20 and 100 $s^{-1}$.

## 4. DISCUSSION

There are some general trends concerning flow stress development regardless of composition. One is that the flow stress at low strains is lower when tested at high strain rate compared to low strain rate tests. The other is that the flow stresses increases more rapidly at high strain rates and ends up at a higher level. This behaviour is reflected in the work hardening behaviour: the level of work hardening is much higher at high strain rates. In addition it is revealed (Figure 6) that the largest improvement in work hardening is at low strains.

The lower flow stress at low strains and high strain rates implies that dislocations move more easily at low strains but accumulates more rapidly in the microstructure and that the microstructure can store more dislocations. Presumably the dislocation density is higher or the subcells smaller at high strain rates. Work hardening is related to the interaction between mobile dislocation and the microstructure. Since generation and annihilation of mobile dislocation is a thermal process, the change from isothermal conditions at low strain rates toward more adiabatic conditions at higher strain rate will affect the mobility and storing of dislocations. An examination of the dislocation structure in TEM is necessary to get a better understanding of these effects.

The flow stress/ work hardening behaviour is consistent with the improvement in ductility. The high level of work hardening at high strain rate gives favourable strain distributions and higher resistance to strain localisation. This explains the increased elongation at higher strain rates.

The effect of alloying elements on the physical behaviour at increasing strain rate is not obvious because of the limited selection of alloys. Some observations are although of interest. The two alloys with additions of Mg and/ or Cu/Zn in solid solution, shows common work hardening behaviour at 20 $s^{-1}$ and 100 $s^{-1}$ (Figure 6), whereas the two alloys which are mainly particulate (the *1200+Fe+Si* and the *1200+Fe+Si+Mn)* display a lower work hardening toward uniform strain at 20 $s^{-1}$ than 100 $s^{-1}$. The same grouping can be made with respect to uniform strain (Figure 4), which increases from $10^{-3}$ to 20 $s^{-1}$ for the solid solution-rich alloys, but are unchanged for the *1200+Fe+Si* and the *1200+Fe+Si+Mn*. There is reason to believe that elements in solid solution in addition to a blend of particle sizes accelerate the high strain rate effects.

## 5. CONCLUSIONS

When increasing the strain rate in selected aluminium alloys from $10^{-3}$ to 20-100 $s^{-1}$, the tested materials display the following features:

* Yielding occurs at lower flow stress. Further increase in strain results in higher levels of flow stress.

* The corresponding improvement in work hardening leads to a considerably higher level of elongation.

* Alloys containing more elements in solid solution experience the high strain rate effects at lower strain rates.

* From a recycling point of view it is encouraging to see that the improvements in properties are most pronounced for the most complex alloys.

* The high level of work hardening at low strains and high strain rates should improve formability of complex parts.

## REFERENCES

[1] J. Gil Sevillano, P.van Houtte, E. Aernoudt : *Prog. Mater. Sci.,* Vol. 25, pp. 69-412 (1981)
[2] R. C. Dorward, K. R. Hasse: *J. Mater. Eng. Perform*, Vol. 4(2), pp.216-220 (1995)
[3] B. Andersson, S. R. Skjervold: *Materials Science Forum,* Vol. 242, pp. 153-158 (1997)
[4] M. F. Shi, D. J. Meuleman: *J. Mater. Eng. Perform*, Vol. 4(3), pp.321-333 (1995)
[5] E. Voce: *J. Inst. metals*, Vol. 74, pp. 537-62 (1948)
[6] A. Considére: *Ann. ponts et chaussées,* Vol. 9, ser 6, pp. 574-775 (1885)
[7] J.E. Hatch: "Aluminium-Properties and Physical Metallurgy". *American Society for Metals (AMS)* (1984)